A Survey of Spin and Relativistic Phenomena in AGN

L.W. Brenneman[1], C.S. Reynolds[2], A.C. Fabian[3], M.A. Nowak[4], R.C. Reis[5], A. Lohfink[2], J.M. Miller[5], K. Iwasawa [6], R. Mushotzky[2], M. Volonteri[7], K. Nandra[8], J.C. Lee[9]

[1]Smithsonian Astrophysical Observatory
[2]University of Maryland
[3]Cambridge University
[4]Massachusetts Institute of Technology
[5]University of Michigan
[6]Institut d'Astrophysique de Paris
[7]Institut de Cincies del Cosmos (ICC), Universitat de Barcelona [8]Max Planck Institute for Extraterrestrial Physics
[9]Harvard University
E-mail(LB): lbrenneman@cfa.harvard.edu

ABSTRACT

Relativistically broadened spectral features have now been seen in the X-ray spectra of many active galactic nuclei (AGN) and Galactic Black Hole Binaries (GBHBs). Investigations of these features allow us to probe the physics of the innermost accretion flow, the geometry of the still-mysterious hard X-ray source, and the spacetime metric of the black hole itself. We conducted a *Suzaku* Key Project (AO4-AO6) that, through very deep observations, has enabled detailed studies of strong gravitational physics in five AGN. This has been the first observational census of supermassive black hole (SMBH) spin ever conducted, and acts as a crucial pathfinder study for one of the principal scientific goals of the *Astro-H* and *ATHENA* missions. In addition to elucidating the role of black hole spin as an energy source in astrophysics, these data have given us our first glimpse at the spin distribution of the local SMBH population. Our deep *Suzaku* observations have yielded spin constraints for three of the five AGN studied, all of which show medium-to-high prograde spin values.

KEY WORDS: galaxies:active — galaxies:Seyfert — X-rays:galaxies — accretion:accretion disks — techniques:spectroscopic

1. Why and How We Measure Black Hole Spin

It has long been recognized that black hole spin may be an important source of energy in astrophysics. Of particular importance is the role that black hole spin is thought to play in relativistic jets such as those seen in radio-loud AGN; the magnetic extraction of the rotational energy of a rapidly spinning black hole is the leading contender for the fundamental energy source of such jets (e.g., Penrose 1969, Blandford & Znajek 1977). The spin distribution of the SMBH population (and its dependence on SMBH mass) also encodes the black hole growth history (Moderski & Sikora 1996; Volonteri et al. 2005, 2007). In essence, if local SMBHs have obtained most of their mass during single disk accretion events (during a quasar phase of activity), we would expect a population of rapidly rotating SMBHs due to the angular momentum accreted from the disks. On the other hand, if SMBH–SMBH mergers or smaller accretion events (King & Pringle 2007) have been the dominant growth mechanism, most of the SMBHs would be spinning at a much more modest rate. So the spin distribution of the local SMBH population gives a new dimension in which models of galaxy and SMBH evolution can be constrained.

We probe strong gravitational physics, including spin, using the relativistically-broadened spectral features that are produced in the surface layers of the inner accretion disk in response to irradiation by the hard X-ray source (Tanaka et al. 1995; Fabian et al. 1995). The most prominent feature in this reflection spectrum is the Fe Kα line. Strong Doppler shifts and gravitational redshifts give this line (and all other features in the reflection spectrum) a characteristic broadened and skewed profile. Since we are really viewing the accretion disk rather than black hole itself, we diagnose black hole spin via its influence on the structure of the disk. The principal effect is due to the spin dependence of the innermost stable circular orbit (ISCO), which is described in detail in the recent reviews of Reynolds (2013) and Brenneman (2013). Simply put, for progressively increasing (prograde) black hole spins, the ISCO and hence the inner edge of the line emitting region are deeper in the black hole potential, and so are subjected to stronger gravitational redshifting. This effect gives the iron line profile the ability to diagnose black hole spin.

At the time of our Key Project this method had already

been successfully applied to determine black hole spin in one AGN (MCG-6-30-15) and several Galactic Black Hole Binaries (GBHBs; Miller et al. 2008ab). The most detailed study of SMBH spin as of 2009 had been conducted by Brenneman & Reynolds (2006; hereafter BR06) using the long 2001 *XMM-Newton* observation of MCG-6-30-15. In spite of the complex absorption present in this AGN, we found the SMBH to be spinning very rapidly, with $a \geq 0.92$, taking into account the systematic uncertainty introduced into this measurement by possible Fe K emission originating from within the ISCO (Reynolds & Fabian 2008). It is important to note, however, that this spin study was made possible with *XMM-Newton*/EPIC data by **assuming** that relativistic reflection produced the Fe K band spectral complexity. Only through studies in the hard X-ray band (most notably with *Suzaku*, but earlier data from *Ginga, BeppoSAX* and *RXTE* made crucial contributions) could we confirm this assumption.

2. Our Suzaku Key Project

We were awarded long observations of five AGN under the auspices of the *Suzaku* Key Project program during cycles AO4-AO6, with the primary goal of searching for and characterizing strong gravity effects —including black hole spin— in these datasets. In order to achieve this goal, great care had to be taken to decompose the relativistic disk spectrum from the effects of intervening absorption (from both neutral and ionized gas) and low-velocity reflection components, making the unique simultaneous, broadband capabilities of *Suzaku* crucial to our success.

Unfortunately, conducting a flux-limited spin survey in SMBHs is not feasible at the current time. Spin measurements require very broadened reflection features corresponding to emission all of the way down to the ISCO, whereas the majority of AGN display comparatively narrow iron lines. Only a modest fraction of X-ray bright, local AGN ($\sim 40\%$, de la Calle Pérez et al. 2010) possess definable X-ray reflection signatures that extend down to the ISCO when observed for sufficiently long integration times. Given the length of observations required to achieve adequate signal-to-noise for studying spin, we chose to target AGN that have already been reported to possess very broadened iron lines on the basis of previous *XMM-Newton* and *Suzaku* observations. The targets, exposure times and details of the observations are presented in Table 1.

We elaborate on the results gleaned from our work on NGC 3783, Fairall 9 and 3C 120 below. Our observations of NGC 3516 and Mrk 841 both display highly complex spectra that result in significant modeling degeneracies between the warm absorber, relativistic reflection and soft excess in these AGN. Work is in progress on these datasets, and they will not be further discussed here.

2.1. NGC 3783

The spectrum of NGC 3783 ratioed against the power-law continuum is shown in Fig. 1. The Compton hump is readily apparent at energies ≥ 10 keV, though its curvature is relatively subtle compared with more prominent features of its kind (e.g., in MCG–6-30-15). The 6-7 keV band is dominated by narrow and broad Fe K features, including a narrow Fe Kα emission line at 6.4 keV and a blend of Fe Kβ and Fe XXVI emission at ~ 7 keV. The broad Fe Kα line manifests as an elongated, asymmetrical tail extending redwards of the narrow Fe Kα line to $\sim 4-5$ keV. At energies below ~ 3 keV the spectrum becomes concave due to the presence of complex, ionized absorbing gas within the nucleus of the galaxy; the gas is ionized enough that some contribution from this absorber is seen at ~ 6.7 keV in an Fe XXV absorption line. There is a rollover back to a convex shape below ~ 1 keV, however, where the soft excess emission dominates. Our initial results and black hole spin constraints are presented in Brenneman et al. (2011; hereafter B11), with follow-up papers exploring the spectral variability (Reis et al. 2012) and systematic uncertainties on the spin (Reynolds et al. 2012).

Brenneman et al. (2011) used a combination of continuum emission (`zpowerlaw`), three zones of warm absorption (XSTAR-generated tables), distant reflection (`reflionx`; Ross & Fabian 2005), and inner disk reflection (`reflionx` convolved with a `kerrconv` smearing kernel; BR06) to fit the 0.7-45 keV *Suzaku* spectrum of NGC 3783 with a statistical quality of $\chi^2/\nu = 917/664\,(1.38)$. Most of the residuals in the best-fit model manifested below ~ 3 keV in the region dominated by the warm absorber and soft excess, as is typical for type 1 AGN. Because the signal-to-noise of the XIS detectors is highest at lower energies due to the higher collecting area there, small residuals in the spectral modeling of this region can have an exaggerated effect on the overall goodness-of-fit. Excluding energies below 3 keV in the fit, B11 achieved $\chi^2/\nu = 499/527\,(0.95)$. No significant residuals remained. See Fig. 1 for the relative contributions of the various model components. The best-fit parameters of the black hole/inner disk system included a spin of $a \geq 0.98$ (down to $a \geq 0.92$ when systematic uncertainties were included), a disk inclination angle of $i = 22^{+3\circ}_{-8}$ to the line of sight, a disk iron abundance of Fe/solar $= 3.7 \pm 0.9$ and an ionization of $\xi \leq 8\,\mathrm{erg\,cm\,s^{-1}}$ (errors are quoted at 90% confidence for one interesting parameter). These parameters remained consistent, within errors, when energies ≤ 3 keV were ignored in the fit, negating the importance of the soft excess emission in driving the fit to these parameter values.

The results of B11 were corroborated by Reis et al. (2012), who examined the temporal and spectral variability of NGC 3783 within the *Suzaku* observation, and by Reynolds et al. (2012, hereafter R12), who re-examined the time-averaged data using a Markov Chain Monte Carlo (MCMC) analysis to more closely probe the total available parameter space. However, Patrick et al. (2011; hereafter P11) analyzed

AGN	z	F_{2-10} ($10^{-12}\,\mathrm{erg\,cm^{-2}\,s^{-1}}$)	$EW_{\mathrm{K}\alpha}$ (eV)	Time (ks)	Counts
NGC 3783	0.0097	60	263	210	626,000
NGC 3516	0.0088	13	300	217	214,000
Fairall 9	0.0470	24	215	191	645,000
Mrk 841	0.0360	11	141	238	313,000
3C 120	0.0330	47	75	140	537,000

Table 1. Observation details from the XIS-FI spectra of our sample of five AGN. The counts were collected from 2-10 keV.

the same data separately and reached a strikingly different conclusion regarding the spin of the black hole in NGC 3783: $a \leq 0.31$. This discrepancy illustrates the importance of assumptions and modeling choices in influencing the derived black hole spin and other physical properties of the black hole/disk system. P11 made three critical assumptions that differed from B11: (1) that the iron abundance of the inner disk is fixed to the solar value; (2) that the warm absorber has a high-turbulence ($v_{\mathrm{turb}} = 1000\,\mathrm{km\,s^{-1}}$), high-ionization ($\xi \sim 7400\,\mathrm{erg\,cm\,s^{-1}}$) component not reported by B11; (3) that the soft excess originates entirely through Comptonization, with the Comptonizing medium at a temperature of $kT \geq 9.5$ keV and an optical depth of $\tau = 1.9 \pm 0.1$.

R12 demonstrated that fixing the iron abundance at the solar value significantly worsens the global goodness-of-fit in NGC 3783 when compared with allowing the iron abundance of the inner disk to fit freely ($\Delta\chi^2 = +36$). R12 also attempted several different model fits to the soft excess and found not only a much smaller contribution to the overall model for the soft excess component than P11, but also no statistical difference between fits using different models (e.g., blackbody vs. `compTT`). It should be noted, however, that modeling the soft excess with a Comptonization component of high temperature, high optical depth and high flux, as P11 have done, requires the `compTT` component to possess significant curvature up into the Fe K band, reducing the need for the relativistic reflector to account for this same curvature seen in the data and thereby eliminating the requirement of high black hole spin. To illustrate this, see Fig. 1 for a plot of the relative importance of the best-fit model components in the P11 vs. B11 analyses. Clearly, different modeling approaches can lead to vastly different conclusions regarding black hole spin and careful consideration should be given to the models used and to their allowed parameter ranges.

2.2. Fairall 9

As we have seen in the cases of MCG–6-30-15 and NGC 3783, spectral complexities like ionized absorption intrinsic to the AGN can confuse our interpretation of the spectrum. It would therefore be ideal to fit relativistic reflection models to a cleaner AGN system without warm absorption as a kind of control case.

There exists a small sample of type 1 AGN, known as "bare" Seyferts, which seem to lack any observable signatures of significant intrinsic absorption in X-rays. While most of these objects do display a soft excess, usually the flux of this component is substantially smaller than that seen in NGC 3783, so the exact model used to parametrize it will have a negligible effect on the spectrum in the Fe K band and will not compromise the spin measured from the broad Fe Kα line and Compton hump. Fairall 9 is one such bright, nearby ($z = 0.047$), "bare" Seyfert with over 160 ks of data in the *XMM-Newton* archive and nearly 400 ks in the *Suzaku* archive. Though a spectral analysis of the *XMM-Newton* data incorporating relativistic reflection features was reported in Brenneman & Reynolds (2009), the first spin measurement for this AGN was published by Schmoll et al. (2009) using a 167 ks *Suzaku* observation from 2007. The spin measured was $a = 0.65^{+0.05}_{-0.05}$, significantly less ($> 6\sigma$) than the high spin values measured for MCG–6-30-15 and NGC 3783, and perhaps indicative of a different galaxy and SMBH evolution history in Fairall 9 than for these AGN.

Our *Suzaku* observation of Fairall 9 was obtained in 2009, and all four *XMM-Newton* and *Suzaku* pointings have recently been analyzed jointly in Lohfink et al. (2012; hereafter L12). Both *Suzaku* pointings are also discussed in P11. By considering all four epochs of data, L12 note that, in spite of the flux variation, the spectral shape remains very similar, with the power-law and distant reflector evident along with a broad Fe Kα line and a noticeable Compton reflection hump above 10 keV. While most of the variation in the flux is due to changes in the power-law strength, a variable soft excess is also visible below 2 keV (see Fig. 2). L12 also note the presence of ionized emission lines of Fe XXV and Fe XXVI in the 2009 *Suzaku* spectrum, which are reported in the *XMM-Newton* observations (Brenneman & Reynolds 2009) but not robustly seen in the 2007 *Suzaku* pointing, according to Schmoll et al. (2009). L12 do report these features in the 2007 data, however.

The best-fitting model obtained by L12 to the four datasets for Fairall 9 requires the standard power-law continuum and near-constant distant reflection plus reflection from an inner accretion disk with sub-solar iron abundance Fe/solar $= 0.67 \pm 0.08$, ranging in ionization from $\xi = 6^{+3}_{-4}\,\mathrm{erg\,cm\,s^{-1}}$

(2007 *Suzaku*) to $\xi = 1739^{+1143}_{-509}\,\mathrm{erg\,cm\,s^{-1}}$ (2009 *Suzaku*). The inclination angle of the disk is measured at $i = 37^{+4\circ}_{-2}$. Additionally, a photoionized plasma is required to explain the ionized iron emission lines seen in the spectrum; this plasma has a loosely constrained ionization of $\xi \sim (0.02 - 10) \times 10^6\,\mathrm{erg\,cm\,s^{-1}}$. The black hole spin is measured at $a = 0.52^{+0.19}_{-0.15}$, consistent with that determined by Schmoll et al. (2009) from the 2007 *Suzaku* data alone. This model yields an excellent goodness-of-fit, with $\chi^2/\nu = 5346/5276\,(1.02)$ (see Fig. 2).

There is still some controversy about the most physically plausible model to use for Fairall 9, however. P11 usea `reflionx` component for both the distant and relativistic reflection, and find that they must also include a neutral absorber intrinsic to the source ($N_\mathrm{H} = 4 \times 10^{23}\,\mathrm{cm^{-2}}$) in order to remove the contribution of the distant reflector from the soft excess emission and fit it adequately with a `compTT` component. There is no clear evidence to either support or disprove the presence of the neutral absorber, which is not reported in any other work on Fairall 9, but it is not necessary to include this component in order to achieve a good fit: the $\chi^2/\nu = 929/881\,(1.05)$ of P11 is comparable to that of L12. It should also be noted that P11 choose to fix the iron abundance of Fairall 9 at $\mathrm{Fe/solar} = 2$, contrary to their approach for the other four AGN in their sample which have $\mathrm{Fe/solar} = 1$.

The `compTT` soft excess used by P11 has a modest flux and optical depth, with $F_{0.6-10} = (3.6 \pm 0.2) \times 10^{-11}\,\mathrm{erg\,cm^{-2}\,s^{-1}}$ and $\tau = 0.5^{+1.6}_{-0.2}$, but the upper limit on its temperature is quite high: $kT < 14.1$ keV. This large temperature pushes the influence of this component almost into the Fe K band, possibly interfering with the measurement of the red wing of the broad Fe Kα line by the `kerrconv` inner disk reflection model. Adopting these assumptions, the authors cannot constrain the spin of the SMBH in Fairall 9 using the dual reflector model, though they do achieve constraints using a more phenomenological approach by modeling the broad Fe Kα line alone with a `kerrdisk` component: $a = 0.67^{+0.10}_{-0.11}$.

Given the differences between the various modeling approaches used in L12 and P11, it is somewhat surprising that the spin constraints achieved in each case are consistent, within errors. This could be an indication that the presence of warm absorption is the greatest complicating factor in measuring spin, due to the curvature it induces in the spectrum interfering with the isolation of the red wing of the broad Fe Kα line. Alternatively (or perhaps in addition to this point), the nature of the spin parameter space could be playing a role in the similarity of the two measurements; the shape of the function relating spin to the ISCO radius changes quite slowly and nearly linearly at moderate spin values below $a \leq 0.9$, but changes much more rapidly above $a \geq 0.9$. Therefore, differentiating between a spin of, e.g., $a = 0.4$ and $a = 0.7$ is much more challenging, statistically, than differentiating between spins of $a = 0.9$ and $a = 0.95$.

2.3. 3C 120

3C 120 was chosen for our sample both because it is one of the few X-ray bright, RLAGN with historical observations of a broad Fe Kα line (e.g., Reeves et al. 2006), and because it has shown evidence for "dips" in its X-ray light curve that are followed by ejections of new plasma at the base of the jet seen in radio observations (Marscher et al. 2002, Chatterjee et al. 2009). The X-ray emission in broad line radio galaxies (BLRGs) is thought to be dominated by the corona of the inner accretion disk (e.g., Marshall et al. 2009). As such, this X-ray/radio connection demonstrates a physical link between changes in accretion disk structure and powerful jet ejection events. This behavior, which is analogous to that seen in Galactic microquasars, is one of the few observational clues that we have to the origin of radio jets.

A 2003 *XMM* observation analyzed by Ballantyne et al. (2004) and Ogle et al. (2005) showed that the X-ray spectrum of 3C 120 above 3 keV can be well described by a power-law and distant reflection, though neutral absorption intrinsic to the source must also be accounted for. Both groups also identified a soft excess, which can be described equally well by bremsstrahlung emission or a second power-law. Kataoka et al. (2007) used *Suzaku* data from 2006 and found indications for relativistic disk emission in the X-ray spectrum. These were confirmed by Cowperthwaite & Reynolds (2012), who found evidence for a truncation of the accretion disk in a re-analysis of the same data set with updated models and calibration.

The addition of our two 2012 *Suzaku* observations, which were performed in conjunction with *Swift* and ongoing VLBA monitoring, enabled us to construct a more holistic picture of the inner regions of 3C 120 and how the source (and, specifically, the broad Fe Kα line) varies over time within the paradigm of the jet cycle. Using multi-epoch disk+jet modeling of the *XMM* and *Suzaku* spectra and placing the X-ray observations in the context of the UV and radio data, L13 were able to fix the spin of the black hole, inclination of the inner disk and iron abundance of the disk while letting the other parameters vary in order to effectively increase the signal-to-noise of the data (see Fig. 3). This approach resulted in the discovery that the *XMM* and *Suzaku* spectra could be described by a black hole spin of $a \geq 0.95$ with the inner disk radius at $r_\mathrm{in} \leq 2\,r_\mathrm{g}$ in *XMM* (2003) and at $r_\mathrm{in} = 40 \pm 20\,r_\mathrm{g}$ in *Suzaku* (2012). The components of the model and their variation between observations are shown in Fig. 3. The *XMM* observation occurred ~ 20 days prior to a new jet knot being observed, while the *Suzaku* observations occurred ~ 10 days after such an ejection event was detected in the radio data.

The optical/UV flux measured by *Swift*/XRT+UVOT exceeds the X-ray flux by a factor of $10-20$ in the 2012 *Suzaku* observations. The existence of a broadband spectral component extending from the optical/UV into the soft X-ray band is supported by the detection of a correlation between the UV/optical and soft X-ray flux within the *XMM* pointing

as well (Ogle et al. 2005). This component may be interpreted as a contribution from the jet (e.g., León-Tavares et al. 2010), which implies that the variability seen is caused by the passage of a new jet component through a stationary feature in the inner jet. A weak correlation between the UV and soft X-ray bands has also been found previously by Maraschi et al. (1991) from simultaneous *IUE-EXOSAT* observations. If modeled with a Comptonization component, this correlation implies physical parameters for the soft excess in 3C 120 similar to those recently discovered in other bright Seyferts (L12; Petrucci et al. 2004), while at the same time ruling out a soft excess arising solely from inner disk reflection.

3. Summary and Future Work

Our *Suzaku* Key Project has produced five deep, legacy-quality datasets of bright, nearby AGN for the mission archive that will bear fruit for years to come. Of these five sources, we have successfully measured the black hole spin of NGC 3783 for the first time at $a \geq 0.92$, we have confirmed previous results indicating that Fairall 9 has an intermediate spin value at $a = 0.52^{+0.19}_{-0.15}$, and we have also provided the most accurate, precise constraint to date on a RLAGN in 3C 120: $a \geq 0.95$. All measurements take systematic errors into account. This project sowed the seeds for the current sample of roughly 22 AGN that have robust constraints placed on the spins of their SMBHs (Reynolds 2013, Brenneman 2013 and sources therein). The distribution of measured spin values is weighted heavily toward prograde, rapidly spinning black holes, with 15/22 AGN having SMBH spins of $a \geq 0.9$. No AGN have yet been seen to harbor non-spinning or retrograde black holes. It is unclear whether these findings are indicative of a true spin bias in local AGN, or whether this observed bias is a function of our sample of AGN and its inherent limitations (e.g., our restriction to performing this science on only very bright sources). Much work remains to be done on this topic, and the sample size of SMBH spins must be increased before any statistical inferences can be drawn about the true distribution of SMBH spins and its implications.

Our Key Project has also shed new light on the nature of the soft excess in AGN and the different physical processes that contribute to it. Though jet emission, scattered emission from the AGN itself, thermal plasma and/or photoionized emission lines from circumnuclear starburst, Comptonization and ionized reflection are all potential contributors (e.g., Crummy et al. 2006, L12), it is becoming clear that no single process can uniquely explain the soft excess in most of the sources that have been studied thus far. Broadband X-ray and UV observations are imperative for studying this spectral component and assesing its origin, since the choice of soft excess model can affect the spectrum out to energies ≥ 30 keV in some cases. Multi-epoch and time-resolved spectral analyses are also critical for understanding the variability (or lack thereof) of this component, yielding additional clues as to its genesis.

Astro-H and *ATHENA* will contribute greatly to this science in the coming decades. The broadband X-ray energy coverage and enhanced spectral resolution of *Astro-H* will prove invaluable for breaking modeling degeneracies between distant and inner disk reflection, and for characterizing the nature of the absorption and soft excess in these AGN. The large effective area of *ATHENA* will allow us to probe out to fainter fluxes than we can with current instruments, increasing the sample size of AGN for which spin measurements can be made. These observatories, coupled with theoretical advances in modeling the various emission and absorption mechanisms in AGN, will pave the path for an improved understanding of how SMBHs and their host galaxies grow and evolve over cosmic time.

References

Ballantyne D. et al. 2004, MNRAS, 354, 839.
Blandford R.D. & Znajek R.L. 1977, MNRAS, 179, 433.
Brenneman L.W. 2013, SpringerBrief in Astronomy, ISBN 978-1-4614-7770-9.
Brenneman L.W. & Reynolds C.S. 2006, ApJ, 652, 1028.
Brenneman L.W. & Reynolds C.S. 2009, ApJ, 702, 1367.
Brenneman L.W. et al. 2011, ApJ, 736, 103.
Chatterjee R. et al. 2009, ApJ, 704, 1689.
Cowperthwaite P.S. & Reynolds C.S. 2012, ApJ, 752L, 21.
Crummy J. et al. 2006, MNRAS, 365, 1067.
Fabian A.C. et al. 1995, MNRAS, 277L, 11.
Kataoka J. et al. 2007, PASJ, 59, 279.
King A.R.& Pringle J.E. 2007, MNRAS, 377L, 25.
León-Tavares J. et al. 2010, ApJ, 715, 355.
Lohfink A.M. et al. 2012, ApJ, 758, 67.
Lohfink A.M. et al. 2013, ApJ, 772, 83.
Maraschi L. et al. 1991, ApJ, 368, 138.
Marscher A. et al. 2002, Nature, 417, 625.
Marshall K. et al. 2009, ApJ, 696, 601.
Miller J.M. et al. 2008a, ApJ, 679L, 113.
Miller J.M. et al. 2008b, ApJ, 680, 1359.
Moderski R. & Sikora M. 1996, MNRAS, 283, 854.
Ogle P.M. et al. 2005, ApJ, 618, 139.
Patrick A.R. et al. 2011, MNRAS, 416, 2725.
Penrose R. 1969, NCimR, 1, 252.
de la Calle Pérez I. et al. 2010, A&A, 524A, 50.
Petrucci P.O.et al. 2004, NuPhS, 132, 213.
Reeves J.N. et al. 2006, AN, 327, 1079.
Reis R.C. et al. 2012, ApJ, 745, 93.
Reynolds C.S. 2013, SSRv, arXiv:1302.3260.
Reynolds C.S. & Fabian A.C. 2008, ApJ, 679, 1159.
Reynolds C.S. et al. 2012, ApJ, 755, 88.
Ross R.R. & Fabian A.C. et al. 2005, MNRAS, 358, 211.
Schmoll S. et al. 2009, ApJ, 703, 2171.
Tanaka Y. et al. 1995, Nature, 375, 659.
Volonteri M. et al. 2005, ApJ, 620, 69.
Volonteri M. et al. 2007, ApJ, 667, 704.

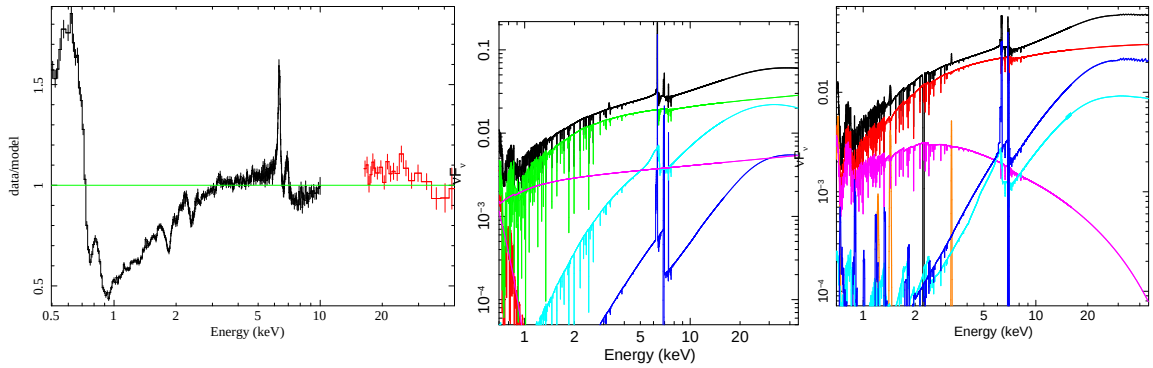

Fig. 1. *Left: Suzaku* XIS-FI (front-illuminated; black) and PIN (red) data from the 210 ks observation of NGC 3783 in 2009, ratioed against a simple power-law model for the continuum (fit over 2 – 4.5 and 7.2 – 10 keV) affected by Galactic photoabsorption. Black and red solid lines connect the data points and do not represent a model. The green line depicts a data-to-model ratio of unity. Data from the XIS back-illuminated CCD (XIS-BI) are not shown for clarity. *Middle:* Relative contributions of the various model components for the B11 best-fit to NGC 3783. Shown are the total model (black), power-law continuum (green), blackbody soft excess (red), scattered emission (magenta), distant reflection (dark blue) and inner disk reflection (light blue). *Right:* Relative contributions of the various model components for the P11 best-fit to NGC 3783. Shown are the total model (black), power-law continuum (red), `compTT` soft excess (magenta), distant reflection (dark blue) and inner disk reflection (light blue). Photoionized emission lines are in orange. Figures are from B11, B11 and P11, respectively.

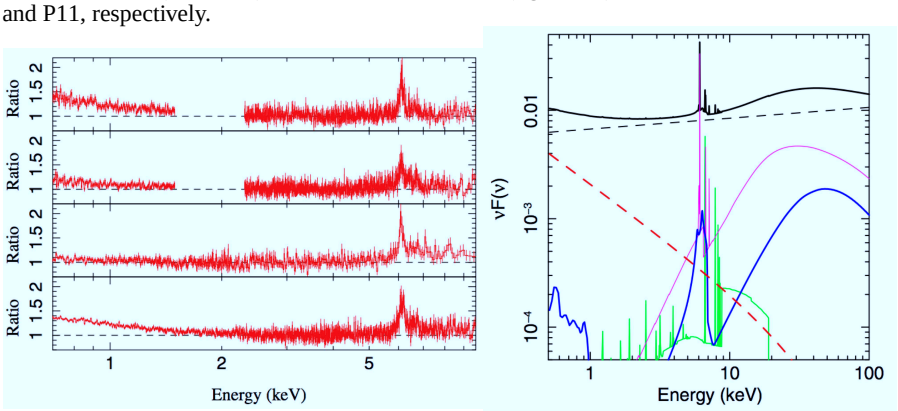

Fig. 2. *Left:* Data-to-model ratios of the Fairall 9 spectra to a simple power-law continuum modified by Galactic photoabsorption. From top to bottom, the datasets represented are *Suzaku* 2007, *Suzaku* 2009, *XMM-Newton* 2009 and *XMM-Newton* 2000. *Right:* Best-fitting model components for the 2007 *Suzaku* data fit by the L12 model including `compTT` emission for the soft excess. Shown are the total model (black solid), power-law (black dashed), inner disk reflector (blue), distant reflector (magenta), and the soft Comptonization component (dashed red). Figures are from L12.

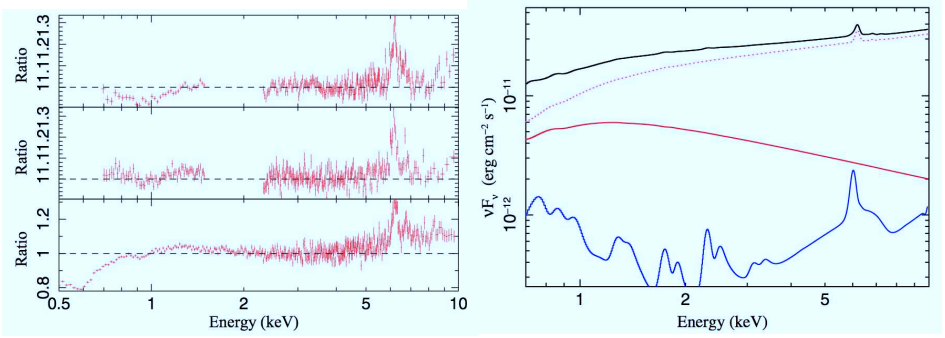

Fig. 3. *Left:* Data-to-model ratio of the *Suzaku*-A (top), *Suzaku-B* (middle) and *XMM* (bottom) observations of 3C 120 to a power-law over the 3-4.5 keV range. Note the change in the Fe K region between pointings. *Right:* Spectral decomposition of the disk+jet model for 3C 120. The solid black line is the total model, dotted red line is the distant reflection+power-law continuum, solid red line is the jet and solid blue line is the contribution from inner disk emission. Figures are from L13.